

Jones, H.L., Westerhold, T., Birch, H., Hull, P., Negra, M.H., Röhl, U., Sepúlveda, J., Vellekoop, J., Whiteside, J.H., Alegret, L., Henahan, M., Robinson, L., van Dijk, J., and Bralower, T., 2022, Stratigraphy of the Cretaceous/Paleogene (K/Pg) boundary at the Global Stratotype Section and Point (GSSP) in El Kef, Tunisia: New insights from the El Kef Coring Project: GSA Bulletin, <https://doi.org/10.1130/B36487.1>.

## Supplemental Material

**Figure S1.** Zoomed-in Google Earth image showing the exact location of the new auxiliary K/Pg outcrop section that was used to guide drilling operations (labeled ‘Survey site’), in relation to the position of the five holes that were drilled during the El Kef Coring Project. Please also note the inferred position of a potential fault (red dashed line) in close proximity to Holes A, D, and E, which may help to explain differences in the stratigraphic thickness of the lower Danian in Holes A, D, and E vs. Holes B and C and (potentially) in Hole D vs. Hole E.

**Figure S2.** Visual comparison of the biostratigraphy in Holes A, D, E and C along the composite depth scale (meters composite depth; mcd). Planktic foraminiferal biozones are shown in boxes and calcareous nannofossil datums are shown to the right of each hole. Bolded numbers are age estimates in Ma for the planktic foraminiferal datums in black (from Wade et al., 2011) and for the calcareous nannofossil datums in blue (from Bernaola and Monechi, 2007). Grey shaded areas represent depth intervals that were not examined for planktic foraminiferal biostratigraphy. Wavy line represents the unconformity. Please note that the unconformity is not lithologically visible in Hole A due to drilling disturbance (cave-in), but is inferred to be located at the displayed depth horizon due to changes in the geochemical signatures (in particular XRF Fe and Zr counts and  $\delta^{13}\text{C}_{\text{org}}$ ), which are consistent with similar changes across the unconformity in Hole E (see Figure 5b, c, and f).

**Figure S3.** Expanded version of Figure 3 showing additional panel with bulk carbonate  $\delta^{18}\text{O}$  data. Line scan images for (a) El Kef A, (b) El Kef D and (c) El Kef E with core numbers and key planktic foraminifer and calcareous nannofossil datums shown to the right of each hole. The relative position of the K/Pg boundary in each hole is shown by a red dashed line. Panels d through h show associated geochemical data from El Kef A (black lines), El Kef D (brown lines), and El Kef E (blue lines) — (d) weight percent total organic carbon (TOC), (e) weight percent calcium carbonate ( $\text{CaCO}_3$ ), (f) bulk organic  $\delta^{13}\text{C}$ , (g) bulk carbonate  $\delta^{13}\text{C}$  and (h) bulk carbonate  $\delta^{18}\text{O}$ . The light blue stars in panels g and h indicate additional stable isotope data that were collected at Yale University; all other data in these panels were collected at the National Oceanography Centre Southampton. Data is plotted against meters below surface (mbs) for each hole, explaining the mismatch in data between holes.

**Figure S4.** Expanded version of Figure 4 showing additional panel with bulk carbonate  $\delta^{18}\text{O}$  data. Line scan images for (a) El Kef A, (b) El Kef D and (c) El Kef E with core numbers and key planktic foraminifer and calcareous nannofossil datums shown to the right of each hole. The relative position of the K/Pg boundary in each hole is shown by a red dashed line. Panels d through h show associated geochemical data from El Kef A (black lines), El Kef D (brown lines), and El Kef E (blue lines) — (d) weight percent total organic carbon (TOC), (e) weight percent calcium carbonate ( $\text{CaCO}_3$ ), (f) bulk organic  $\delta^{13}\text{C}$ , (g) bulk carbonate  $\delta^{13}\text{C}$  and (h) bulk carbonate  $\delta^{18}\text{O}$ . The light blue stars in panels g and h indicate additional stable isotope data that

were collected at Yale University; all other data in these panels were collected at the National Oceanography Centre Southampton. Data is plotted against meters below surface (mbs) for each hole, explaining the mismatch in data between holes.

**Figure S5.** Multi-Taper-Method spectral analysis results using the El Kef XRF Fe Area data spanning the Maastrichtian interval smoothed by 10pt LOESS smooth and resampled at 1 cm.

Code used in Astrochron:

```
mtmML96(rc,tbw=3,ntap=5,padfac=5,demean=T,detrend=T,medsmooth=0.2,opt=3,linLog=2,siglevel=0.9,output=1,CLpwr=T,xmin=0,xmax=5,sigID=T,pl=2,genplot=T,verbose=T)
```

The broader spectral peak at about 0.28 cycles per meter is equivalent to 3.5 m cycle thickness. Please keep in mind that the Maastrichtian record is only 5 cycles, being at the edge of what can be done and is statistically meaningful.

**Figure S6.** Gaussian filter of the El Kef XRF Fe Area data spanning the Maastrichtian interval with central frequency 0.28 and 30% bandwidth of 0.084. About five cycles are reconfirmed by spectral analysis.

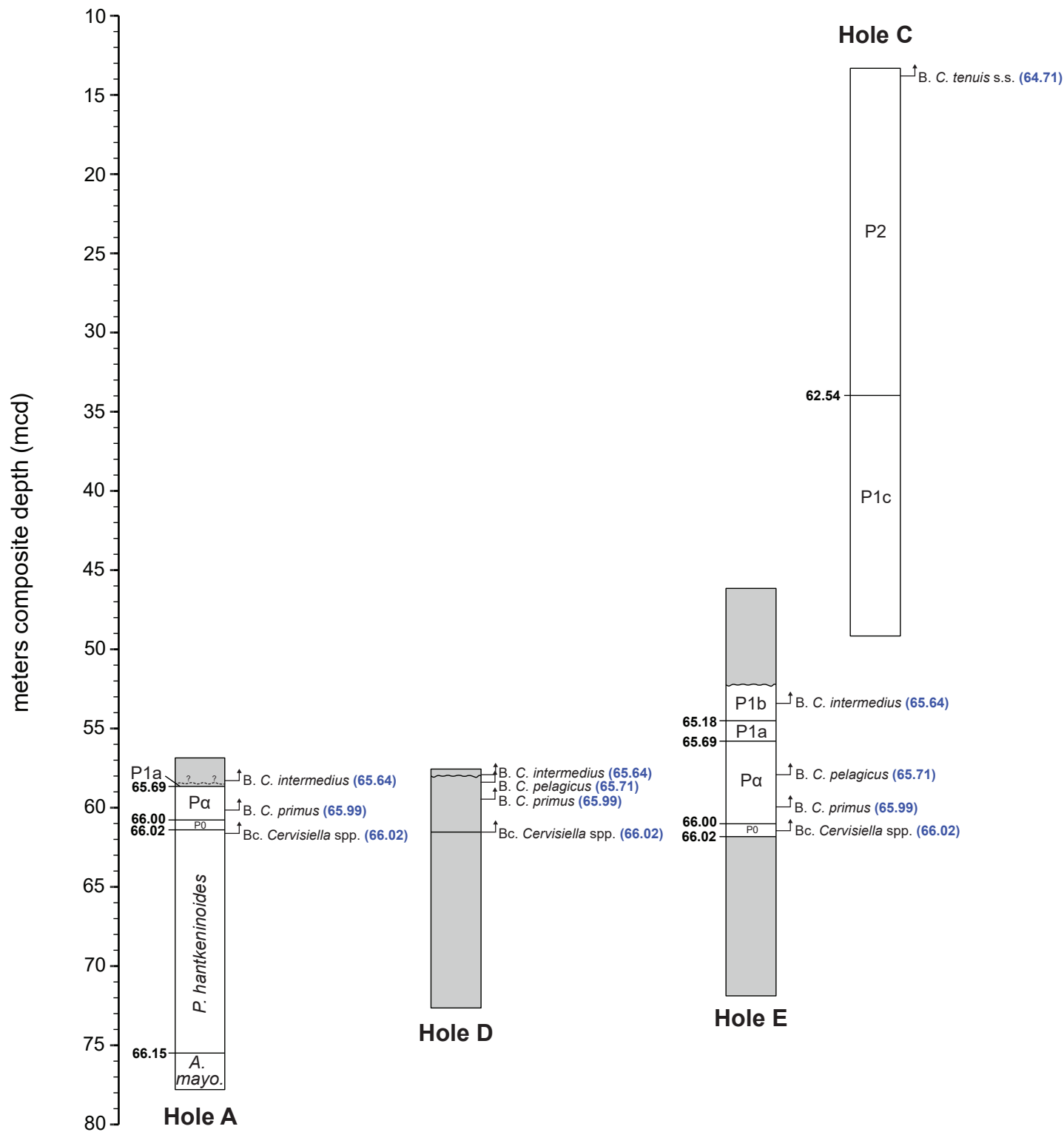
**TABLE S1.** MODIFIED AGE MODEL OF OCEAN DRILLING PROGRAM (ODP) SITE 1262: WALVIS RIDGE (WESTERHOLD ET AL., 2020)

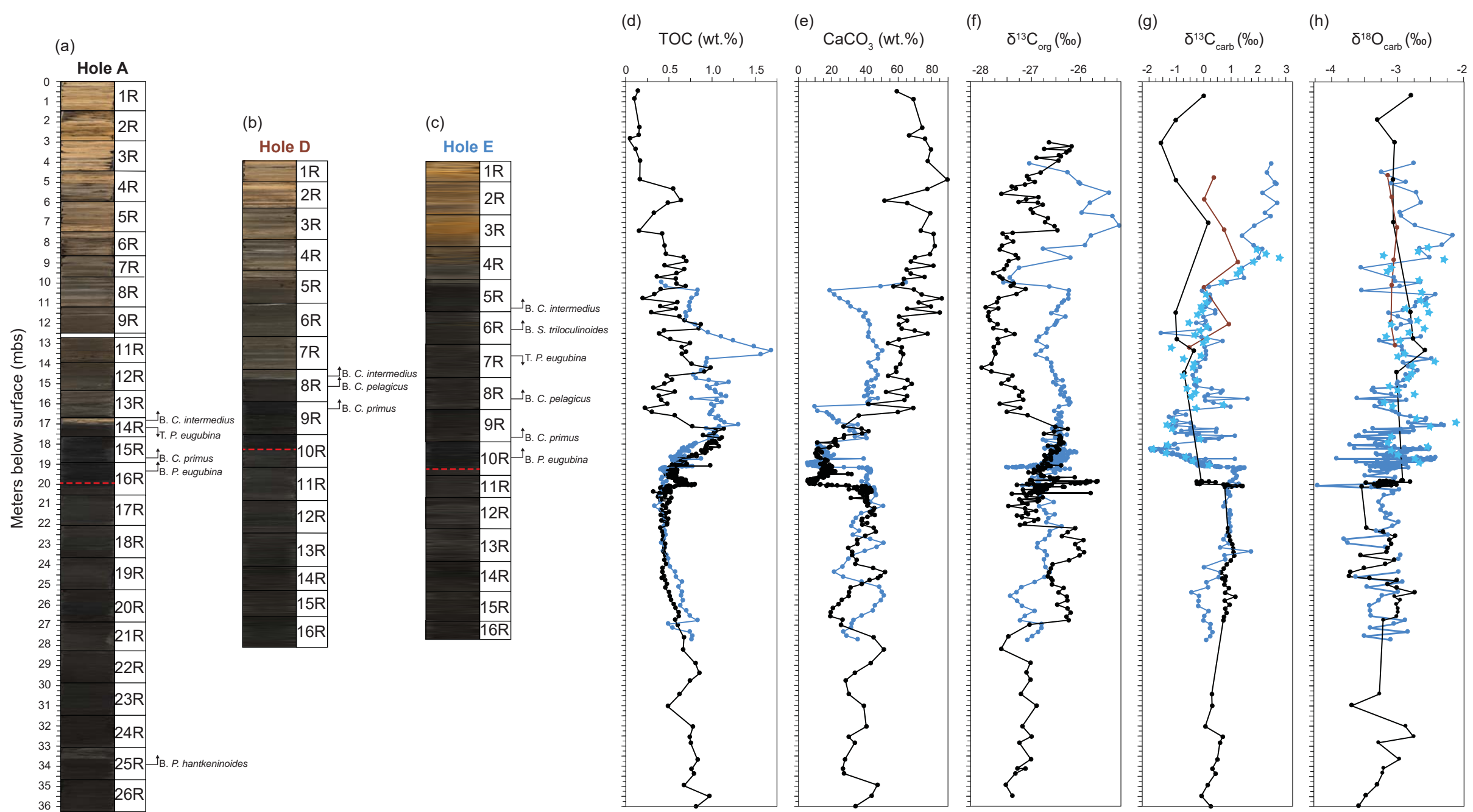
**TABLE S2.** CORRELATION OF EL KEF CORES TO ODP SITE 1262 USING FE MAXIMA

**Data S1.** [\[\[Caption?\]\]](#)

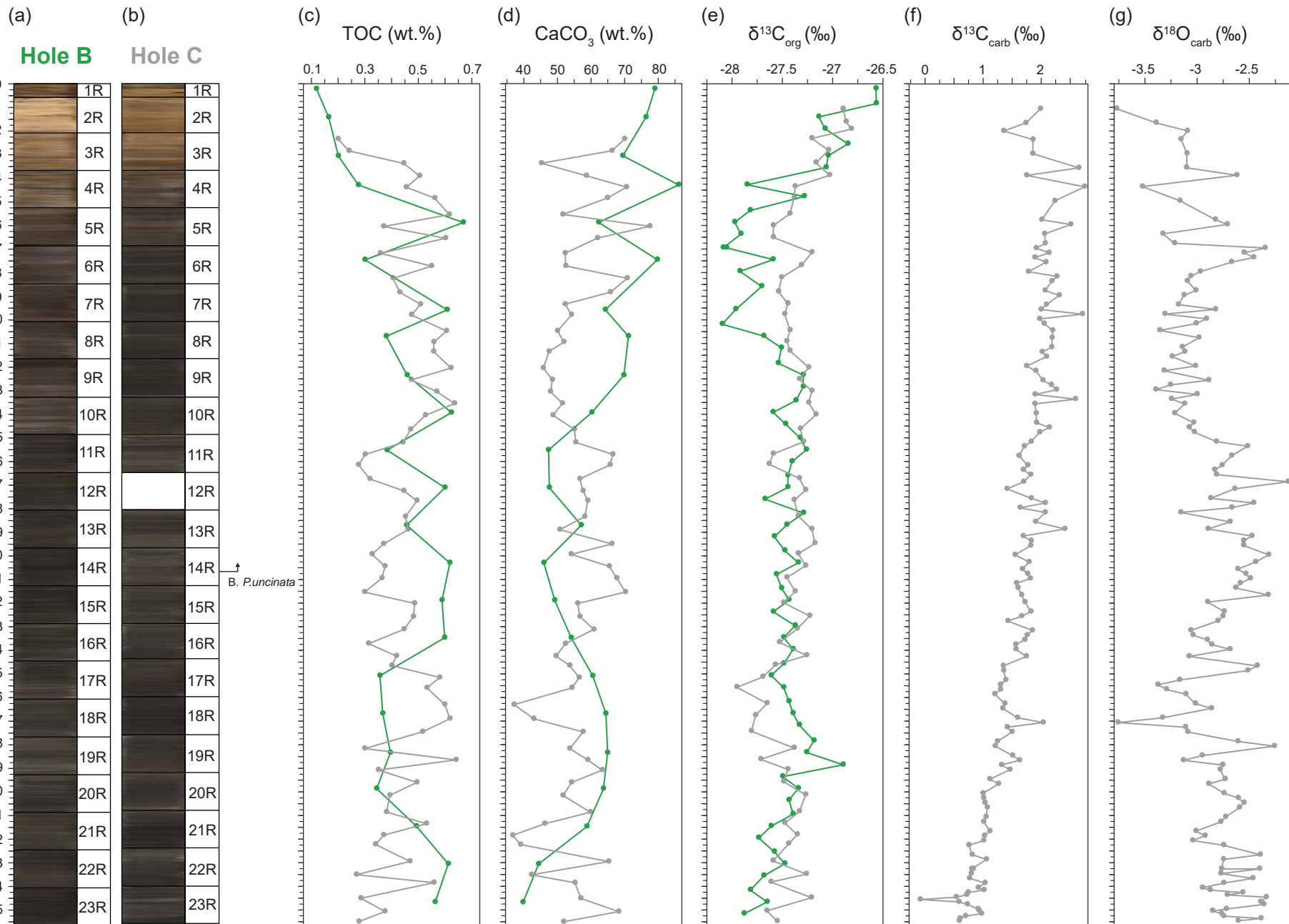
**Data S2.** [\[\[Caption?\]\]](#)





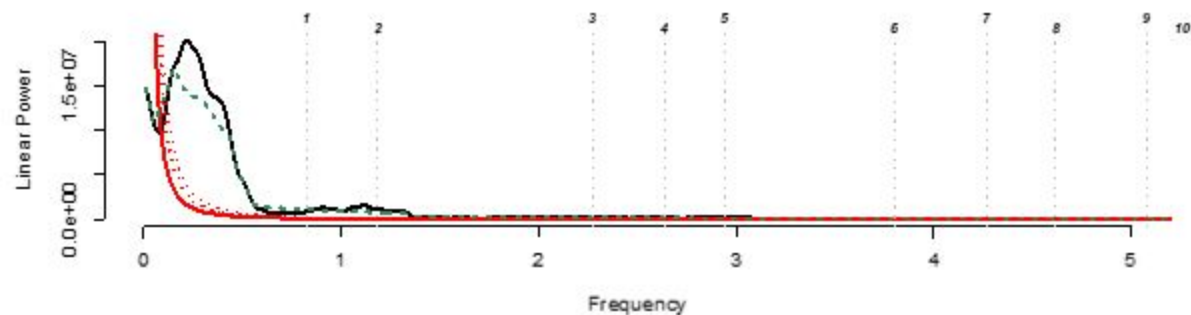


Meters below surface (mbs)

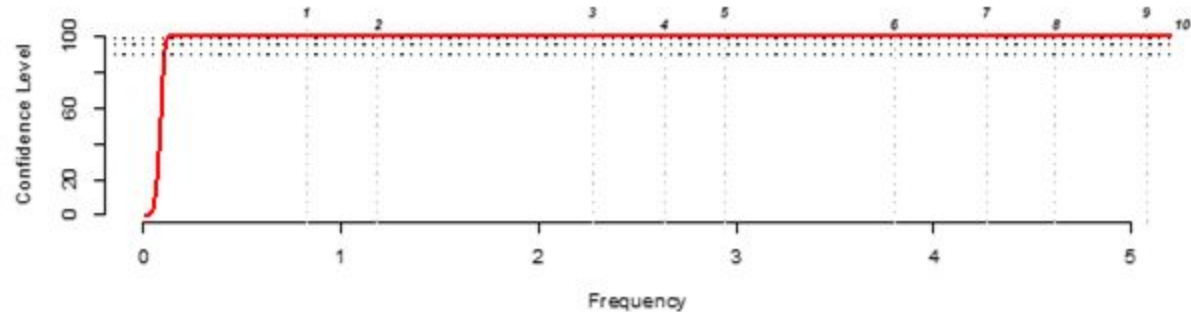




MTM Power (black), Robust AR1 fit (red), smoothed (green)



Robust AR1 Confidence Level E estimates



MTM Harmonic F-test Confidence Level Estimates

